frontiers in Materials

ORIGINAL RESEARCH
published: 30 April 2019
doi: 10.3389/fmats.2019.00096

Sol-gel Synthesis of TiO_2 With p-Type Response to Hydrogen Gas at Elevated Temperature

Lijuan Xie[1,2], *Zhong Li*[1,2*], *Linchao Sun*[1,2], *Baoxia Dong*[3], *Qawareer Fatima*[1,2], *Zhe Wang*[1,2], *Zhengjun Yao*[1,2] *and Azhar Ali Haidry*[1,2*]

[1] College of Materials Science and Technology, Nanjing University of Aeronautics and Astronautics, Nanjing, China, [2] Key Laboratory of Materials Preparation and Protection for Harsh Environment, Ministry of Industry and Information Technology, Nanjing, China, [3] College of Chemistry and Chemical Engineering, Yangzhou University, Yangzhou, China

Titanium dioxide is considered as one of the potential candidates for high-temperature gas sensing applications due to its excellent sensitivity and stability. However, its practical use as a gas sensor under elevated conditions is limited on account of its selectivity and insufficient understanding of response conversion from n- to p-type. To this context, the present work is intended to prepare and understand the p-type response of anatase TiO_2 toward H_2 gas (20–1,000 ppm) at elevated temperature (500°C). Sol-gel route is adopted to facilely synthesize powders containing pure and chromium (1–10 at.%) doped TiO_2 nanoparticles, which are then brushed onto substrates with already patterned inter-digitated platinum electrodes. In this work, even, the undoped TiO_2 samples showed p-type gas sensing response, which then decreased with Cr doping. However, in comparison to previously reported work, the sensing characteristics of all sensors is improved. For instance, 5 at.% Cr-TiO_2 showed high response (147), fast response and recovery (142/123s) time, and good selectivity to hydrogen against monoxide and methane. Despite better response values, the TiO_2 based samples show instability and drift in baseline resistance; such issues were not observed for Cr-doped TiO_2 samples (≥3 at.%). The powders were further analyzed by XRD, SEM, TEM, and XPS to understand the basic characteristics, p-type response and stability. Further, a plausible sensing mechanism is discussed on basis of results obtained from aforementioned techniques.

Keywords: sol-gel method, Cr doped TiO_2, nanoparticles, hydrogen sensitivity, high temperature

OPEN ACCESS

Edited by:
Kalisadhan Mukherjee, Pandit Deendayal Petroleum University, India

Reviewed by:
Tarapada Sarkar, University of Maryland, College Park, United States
Shyambo Chatterjee, University of Nebraska-Lincoln, United States

***Correspondence:**
Zhong Li
nuaalizhong@163.com
Azhar Ali Haidry
aa.haidry@nuaa.edu.cn

Specialty section:
This article was submitted to Functional Ceramics, a section of the journal Frontiers in Materials

Received: *25 February 2019*
Accepted: *15 April 2019*
Published: *30 April 2019*

Citation:
Xie L, Li Z, Sun L, Dong B, Fatima Q, Wang Z, Yao Z and Haidry AA (2019) Sol-gel Synthesis of TiO_2 With p-Type Response to Hydrogen Gas at Elevated Temperature. Front. Mater. 6:96. doi: 10.3389/fmats.2019.00096

INTRODUCTION

Expected to be widely used energy source in the near future, hydrogen has gained increasing attention as one of the cleanest energy sources. However, its use in practical applications is limited because, during production, storage, transportation and use, H_2 can effortlessly leak out as the atomic distance between the centers of two hydrogen atoms in H_2 molecules is very small (~1.06 Å). Refer to the lower and upper explosive limit (LEL-UEL~4.0–75.0), H_2 gas possesses flammable and explosive nature when leaked and, subsequently, mixed with oxygen from the surrounding air. As a consequence, explosion caused by hydrogen leakage presents a major threat to not only human but also the environment (Haidry et al., 2012; Hermawan et al., 2018; Li et al., 2018). From this perspective,

it is utmost important to monitor hydrogen in production plants, pipelines, storage tanks, refilling stations and automotive vehicles, specifically at high temperature. Thus, it is urgent and worthwhile to develop low-cost sensors to monitor the concentrations of H_2. One of the main challenges in hydrogen sensor working at high temperature is to aim higher sensitivity, selectivity, faster response time with excellent stability.

With the capacity to operate in harsh environment, gas sensors based on metal oxides (MOXs) are one of the potent candidates for hydrogen sensing applications (Bai and Zhou, 2014; Li et al., 2017). Among them, n-type semiconductor titanium dioxide (TiO_2) based gas sensor has attracted the enormous interest of researchers due to its outstanding physical and chemical properties: low cost facile fabrication, non-toxic nature, wide energy gap (E_g = 3.0–3.4 eV), and high sensitivity. Furthermore, the chemical stability of TiO_2 at high temperature make it exquisite contender for high temperature sensing applications (Li et al., 2009; Liu et al., 2014). TiO_2 in nature has three crystal structures, known as brookite, anatase, and rutile; rutile, and anatase are most widely used as a gas sensor. Rutile is more stable at high temperature while anatase has better gas sensitivity due its eminent gas reaction capability (Comini et al., 2005; Li et al., 2009; Jing et al., 2015). Currently, the TiO_2-coatings based on physical vapor deposition (e.g., sputtering) are mainly for high temperature gas sensing, which is carried out under high vacuum, thus increasing the cost of the final device. On the other, the sol-gel method has several advantages, such as facile, low cost, uncomplicated environmental requirements, and mass production.

Although TiO_2 is promising high-temperature gas sensitive material, it still has several inadequacies, such as low selectivity and surface contamination, reduction and aging in high temperature and harsh environments. Up to now, an accepted strategy to improve metal oxides gas sensor properties is to dope with metals or surface modification with catalytic metals. Metal ions of different valence states act as donors or acceptors in TiO_2, respectively, which can change the electrical conductivity of TiO_2, thereby having effects on the response time and sensitivity (Sennik et al., 2016; Luo et al., 2017; Pan et al., 2018). Chromium, one of the non-noble metals, is suggested to be suited as a dopant for improved TiO_2 sensing applications (Lyson-Sypien et al., 2012; Haidry et al., 2016; Sun et al., 2018; Monamary et al., 2019). The ionic radii of Ti^{4+}(0.60 Å) and Cr^{3+}(0.61 Å) is circa similar, thus Cr^{3+} can replace Ti^{4+} in TiO_2 lattice to form additional defects (as oxygen vacancies and interstitial Ti atoms), which can change the electronic structure of TiO_2 and transform TiO_2 into p-type. Based on its p-type conductivity, Cr^{3+} doped TiO_2 exhibits better sensitivity to H_2.

The ultimate aim of this work is to fabricate hydrogen sensors with high sensitivity that can work stably at high temperatures by simple and cost-effective sol-gel method. The motivation for this study is to improve the stability of TiO_2 based gas sensors at high temperature for hydrogen detection as well as to investigate the sensing mechanism of pure and Cr doped TiO_2 sensing materials. The effect of chromium dopant on the crystallite structure and topography of titanium dioxide was analyzed. The dynamic responses of synthesized sensor at high temperature to hydrogen are also discussed.

MATERIALS AND METHODS

Preparation of Cr-Doped TiO_2

In this work, the nanomaterials based on Cr_XTiO_2 (X = 0, 1, 3, 5, 10 at.%) prepared by sol-gel method. All chemicals used were of analytical grade reagents purchased from commercial channels and were used without any further purification unless mentioned elsewhere. The analytical grade Tetrabutyl titanate ($C_{16}H_{36}O_4Ti$, purity ≥98.0% from Aladdin, abbreviated as TBOT) precursor was used served as the source of titanium. The chromium acetate ($C_6H_9O_6Cr$, purity ≥99.9% from Aladdin) was used as a source of chromium, nitric acid as a chelating agent, acetic acid (CH_3COOH) as a catalysts, and ethanol as a solvent. Firstly, 12 ml TBOT and 1 ml acetic acid were dissolved in 25 ml ethanol in a beaker (named solution A), under continuous stirring at room temperature and ambient pressure for 1 h. The chromium acetate with different atomic contents (1, 3, 5, 10 at.%) and 3 ml DI water were dissolved in 25 ml ethanol in another flask (named solution B). Then, to adjust the pH value of solution B to 1, the nitric acid was added drop-wise under continuous stirring for 30 min. Following, the solution B was added drop-wise into stirred solution A. After stirring for 2 h under ambient condition, homogenous light yellow sol was formed. After aging for 12 h, the gel was dried in an oven for 12 h at 70°C. Afterwards, the obtained powder was grinded and subsequently annealed at 600°C for 1 h in a muffle furnace (HeFei Kejing Materials Teccnology Company) under static air condition. The synthesized TiO_2 and Cr_XTiO_2 (X = 0, 1, 3, 5, 10 at.%) powder were named as TO, TOC1, TOC3, TOC5, TOC10, respectively.

Characterization

The crystal structure analysis of the obtained TiO_2 powder was performed using X-ray diffraction (XRD, Rigaku Ultimate IV from Japan) with Cu Ka (λ = 1.5406 Å) and the diffraction angle range 20–80° at a scanning rate 5° min^{-1} The surface morphology of the nanoparticles was investigated using scanning electron microscopy (Hitachi S-4800) from Japan, and the compositions of the materials were determined by energy dispersive spectroscopy (EDS) attached to the SEM. The transmission electron microscopy (TEM) images were obtained by using JEM-2100F transmission electron microscope (JEOL Ltd. Japan). Thermo ESCALAB 250XI X-ray photoelectron spectroscopy (XPS) was performed on the prepared powder to analyze elemental chemical.

Fabrication and Measurement of the Sensors

After annealing at 600°C, the powder was grinded for several hours and then mixed in deionized water to form thick paste. Using a brush, the pastes were coated on alumina substrates having Pt interdigital electrodes. Then, the substrates adhered gas sensing paste was dried in hot plate for 30 min at 80°C.

The gas sensing characteristics were carried out by independent design gas sensing measurement device (Functional

Materials and Chemical Sensor Lab, FuMS). The detailed of the sensing apparatus is already reported elsewhere (Haidry et al., 2018). To measure the resistance change of the sensor, different voltages (0.1, 1, 2 V were applied on the sensors in high operating temperatures (300–500°C) toward different gases (CO, H_2, CH_4). Here, the sensor response (S_R) is defined as the ratio

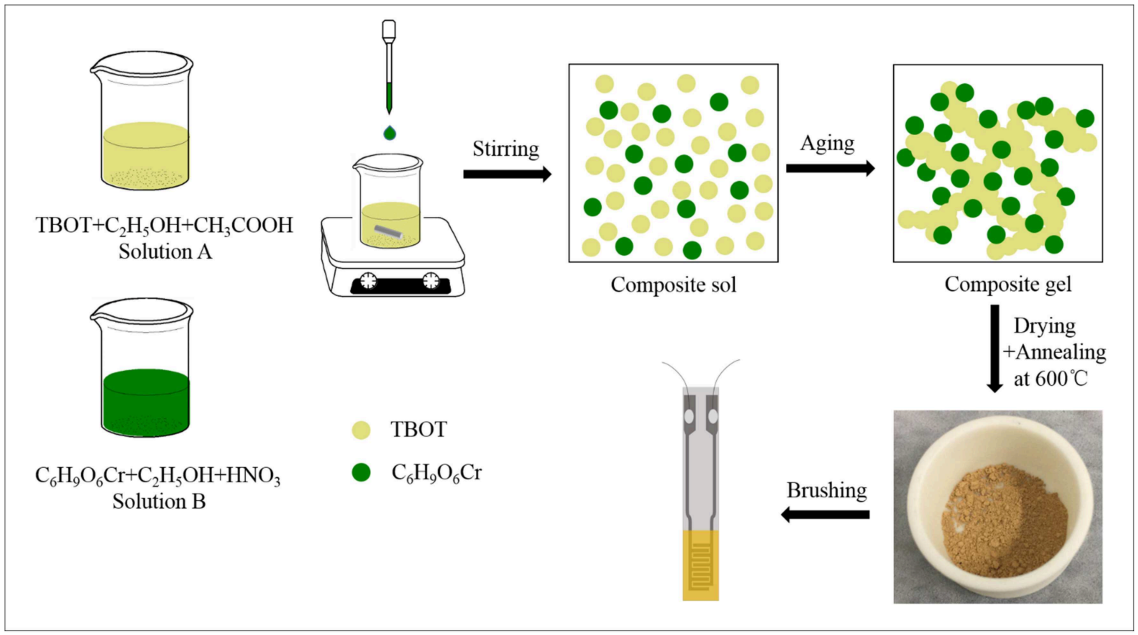

FIGURE 1 | The schematic illustrating the fabrication process of undoped and Cr-doped TiO_2 nanopowders and gas sensors is shown.

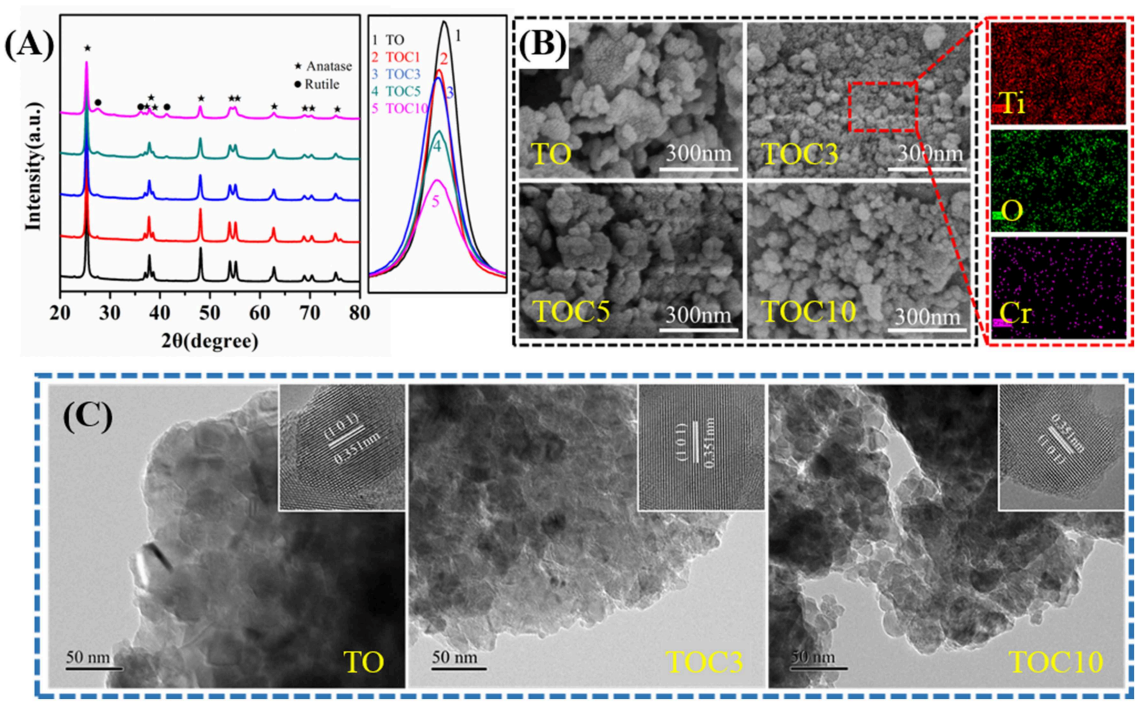

FIGURE 2 | XRD diffractograms **(A)** of TOC, TOC1, TOC3, TOC5, TOC10, and the comparison of anatase (101) peak, SEM micrographs **(B)** of TOC, TOC3, TOC5, TOC10, and elemental mapping of TOC3, TEM, and HRTEM images **(C)** of TO, TOC3, TOC10.

of R_{gas}/R_{air} where R_{air} and R_{gas} are the resistance in dry air and gas, respectively. The response and recovery times are defined as 90% change in the baseline stable resistance, respectively. The selectivity factor (S_F) was estimated as the response ratio of hydrogen against other gases. The typical schematics of the process of Cr doped TiO_2 nanopowders and gas sensors fabrication procedure is shown in **Figure 1**.

RESULTS AND DISCUSSION

Structural and Morphological Characteristics

The structural change of TiO_2 before and after doping Cr was characterized by XRD diffractograms. **Figure 2A** shows the XRD diffractograms of pure and Cr-doped TiO_2 nanoparticles annealed at 600°C. Comparing with the standard XRD patterns of TiO_2 (JCPDS Card 21-1272 and 21-1276), the prepared nanopowders are mainly anatase with a minor amount of rutile phase. The diffraction peaks at 2θ [°] = 25.35, 36.88, 37.78, 38.51, 48.07, 53.92, 55.11, 62.07, 68.59, 70.36, 75.09 are indexed to anatase TiO_2 phases (101), (103), (004), (112), (200), (105), (211), (213), (116), (200), (215), and the peak at 2θ [°] = 27.51, 36.04, 41.19 are indexed to rutile TiO_2 phases (110), (101), and (111). With the increasing Cr contents, the diffraction peaks of rutile become obvious. Thus, it can be concluded that Cr ions can promote the transformation of anatase to rutile when annealed at 600°C. On the basis of the reports (Gonullu et al., 2015), it can be explained by the formation electric stress produced as a result of Cr replacing Ti^{4+} in TiO_2 lattice. Having similar ionic radii with Ti^{4+} (0.60 Å), Cr^{3+} (0.61 Å) can substitute Ti^{4+} without any visible deformation. However, Cr doping forms oxygen vacancies with positive charges and generates electrical stress which facilitates the transformation from anatase to rutile even at 600°C. In this work, no diffraction

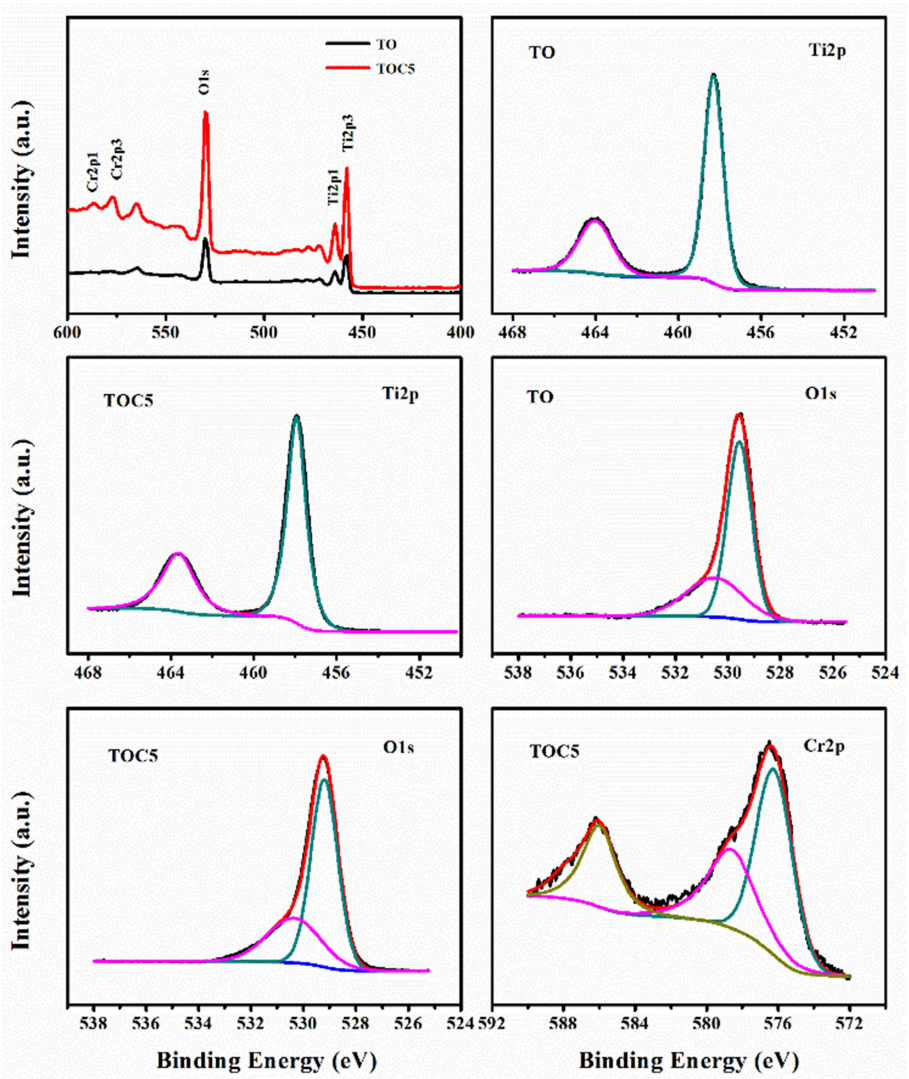

FIGURE 3 | XPS spectra of TO and TOC5, Ti 2p of TO and TOC5, O 1s of TO and TOC5, and Cr 2p of TOC5.

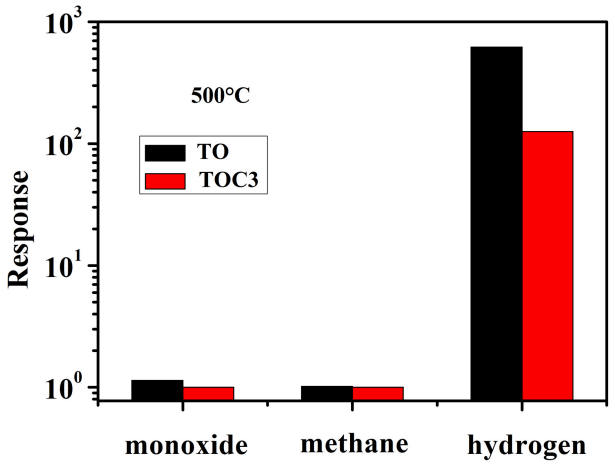

FIGURE 4 | H_2-selectivity of the sensors against monoxide and methane (1,000 ppm).

peaks associated with Cr appear even for the powder having is up to 10 at.% Cr concentration. Thus, it can be speculated that Cr is successfully incorporated into the TiO_2 lattice. According to Scherrer's equation ($D_{XRD} = 0.9\frac{\lambda}{dcos\theta}$), the average crystallite sizes of nanoparticles are 25.1, 24, 23.2, 21.4, 21.3 nm for TO, TOC1, TOC3, TOC5, TOC10, respectively. The results indicate that the crystallite size decreases slightly with the increasing of Cr concentration, which strongly agrees with previous publication (Asemil et al., 2017).

SEM analysis in **Figure 2B** reveal similar microstructure of pure and Cr doped TiO_2. All samples are composed of irregular nanoparticles ranging from 20 to 200 nm, and the nanoparticles are piled up to form loose structure. There is contrasting difference between the XRD and SEM grain sizes since values of TiO_2 grains from XRD means the volume where the crystalline structure is intact. It can be clearly seen from **Figure 2B** that the size of pure TiO_2 particles is bigger than Cr doped TiO_2. The elemental mapping of TOC3 indicates the presence and distribution of Ti, O, Cr elements.

The TEM and HRTEM images of the pure and Cr-doped TiO_2 calcined at 600°C are presented in **Figure 2C**. The aggregation of the nanoparticles is more obviously observed in TEM images. As shown in the images, with the increase of chromium concentration, the aggregation becomes weak and, therefore, it is speculated that Cr dopant can prevent TiO_2 nanoparticles aggregating. The main interplanar crystal spacing value measured from lattice fringes is 0.35 nm, which corresponds to the A (101) plane of the TiO_2. No evidence on spacing on metallic Cr or oxidized Cr was found.

The x-ray photoelectron spectroscopy (XPS) measurements were carried out to investigate the changes in the chemical and electronic states of the elements. The XPS survey and high-resolution spectra of Ti 2p, O 1s, Cr 2p are presented in **Figure 3**. The XPS spectrum of TOC5 reveals Cr, Ti, and O element. The peaks in Ti spectra of TO around 458.3 and 464 eV describe Ti^{4+} 2p3/2 and Ti^{4+} 2p1/2, respectively (Peng et al., 2012), which shift slightly to lower binding energy (∼0.4 eV) in TOC5. The O 1s spectra of TO display overlapping peaks at 529.6 and 530.5 eV, which are attributed to lattice oxygen (Ti-O-Ti) in TiO_2 and surface absorbed oxygen, respectively (Alvarez et al., 2019). These peaks also shift slightly to lower band energy of 529.2 eV and 530.4 eV displayed in TOC5. The Cr 2p3/2 spin-orbital splitting photoelectrons for TOC5 located at binding energies of 576.3 and 586.2 eV, could be assigned to Cr^{3+}, binding energy at 578.6 and 587.9 eV that assigned to Cr^{6+} was also detected (Lacz et al., 2018; Alvarez et al., 2019). The above results prove Cr incorporation into the TiO_2 lattice, which are in good agreement with previous reports (Low et al., 2013; Alvarez et al., 2019).

Gas Sensing Properties

Generally, TiO_2 is n-type but in our case it shows p-type H_2 response. In this work, with the purpose of developing TiO_2 based gas sensors for high temperature application, the sensing measurements were performed at 500°C toward reducing gases monoxide (CO), methane (CH_4), and hydrogen (H_2) firstly. **Figure 4** demonstrates the response S_R of TO and TOC3 sensors to 1,000 ppm of CO, CH_4, and H_2. The selectivity factor S_F of pure TiO_2 for H_2 is ∼543.6 and ∼607.5 against interfering gases CO and CH_4, respectively, indicating the gas sensor exhibits high selectivity to H_2.

For the sensors based on TO, the relationship between the response and operating temperature was studied see **Figure 5A**. Using low applied voltage 0.1 V, the sensor showed much higher response to hydrogen at 500°C. For 1,000 ppm hydrogen, the response ($S_R \sim 619.7$) at 500°C is about 200 times higher than at 300°C ($S_R \sim 3.28$). It is well-known that the sensitivity of metal oxides depends on the temperature and there exist an optimal operating temperature. In a typical case, the sensing response increases with the temperature and after a maximum value it falls. At lower temperature, the energy is not strong enough to overcome the reaction activation energy barrier, leading to a poor sensitivity. However, over the optimal temperature, the accumulation of a large number of heat energy on the surface makes exothermic gas chemisorption difficult and the gas desorption dominate, resulting in reducing response value (Yamazoe and Shimanoe, 2008; Diao et al., 2016). In this work, the optimal temperature was not found. Thus, 500°C is selected as operating temperature and all the following measurements were performed at this temperature except to understand the influence of applied voltage. The influence of applied voltage on the sensitivity was also studied. **Figure 5B** shows the response value of TiO_2 sensor to 50–1,000 ppm hydrogen at 300°C with 0.1, 1, and 2 V. As can be seen in **Figure 5B**, when the applied voltage increases, the sensitivity of the TiO_2 sensor promotes obviously. For instance, the response values are ∼3.28 with ∼82.91 and ∼ 465.18 with 0.1, 1, and 2 V, respectively, toward 1,000 ppm hydrogen.

The real time changes in the electrical resistance R of undoped TiO_2 sensor materials upon interaction with H_2 as a function of time in **Figure 5C** (known as dynamic response) exhibit that the pure TiO_2 sensor yields p-type semiconductor behaviors at all operating temperatures. At 500°C, when the target gas released,

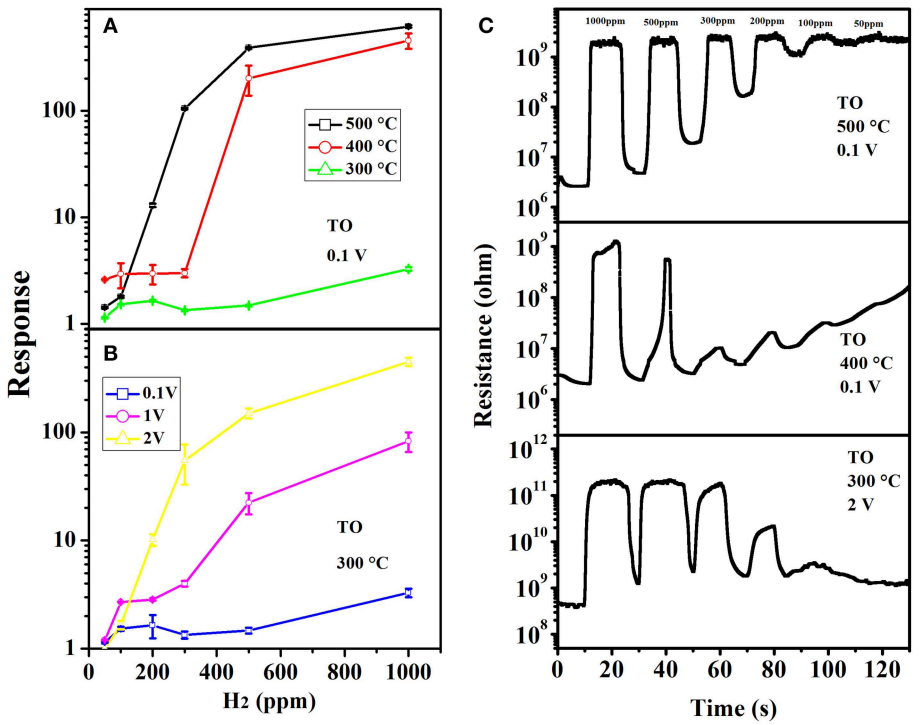

FIGURE 5 | Response values of sensors **(A)** based on TO to 50–1,000 ppm hydrogen at different operating temperatures (300–500°C) with 0.1 V. Comparative response values of sensors **(B)** based on TO to 50–1,000 ppm hydrogen at 300°C with 0.1, 1, and 2 V. The dynamic response curves of sensors **(C)** based on TO vs. 50–1,000 ppm hydrogen at different operating temperatures (300–500°C).

the resistance of the sensor cannot return to the initial value. This phenomenon calls the baseline resistance drift, and with the temperature increases, the baseline resistance drift becomes more severe. To sum up, for TiO_2 sensor, the most suitable working condition is at 300°C with 2 V applied voltage.

The dynamic response curves toward various concentrations of hydrogen ranging from 20 to 1,000 ppm at 500°C with 0.1 V applied voltage are presented in **Figures 6A,B**. The resistance of all sensors increases rapidly when exposed to hydrogen and then decrease when exposed to the background air, which presents the p-type semiconducting gas sensing behaviors. It is clearly illustrated that not only the pure TiO_2 but also lower content Cr doped TiO_2 sensors, when hydrogen is exposed, the resistance of these sensors cannot return to the initial value. Furthermore, the baseline resistance drift notably improves with the increase of Cr concentration; with Cr concentration up to 5 at.%, the resistance drift removes completely. However, when Cr concentration reaches up to 10 at.%, the sensor does not show any response to hydrogen. Therefore, we can conclude that Cr dopant can improve the stability of TiO_2 sensors. The response and recovery time are given in **Table 1**. **Figure 6C** shows the sensing performance of pure TiO_2 and different content Cr doped TiO_2 sensors on 20–1,000 ppm at 500°C. It is found that the response is 619.7, 197.8, 125.8, 147 for TO, TOC1, TOC3, TOC5, respectively, at 500°C under similar conditions as shown in **Figure 6C**. Pure TiO_2 sensors show high sensitivity to all hydrogen concentrations. Responses of pure and Cr doped TiO_2 sensors are further observed to 20–100 ppm of hydrogen in **Figure 6D**. Minimum hydrogen concentration that the fabricated sensor is detecting at 500°C is 20 ppm as can be seen in the **Figure 6B**. It is also noticeable in **Figure 6** that Cr dopant reduces the sensing response of TiO_2 sensors toward hydrogen. Both sensitivity and stability are vital for an excellent gas sensor. Thus, we can select 5 at.% Cr doped TiO_2 sensor as the optimum sensor that can work at high temperature considering all factors.

Sensing Mechanism

The gas-sensing characteristics of p-type and n-type semiconductors are notably different in the context of the resistance variation during targeting gas exposure. Taking n-type semiconductors as an example, the oxygen molecules get trapped by taking electrons from conduction band near the surface that leads to the formation of negatively charged chemisorbed oxygen species, such as O_2^-, O^-, and O^{2-} in the flow of air, see Equations (1–3). Upon exposing to the reducing gas, the trapped electrons are subsequently released back to TiO_2-surface due to interaction between the target gas and adsorbed oxygen species. This reaction reduces the thickness of space charge region (depletion layer) resulting an increase of surface conduction electron density [e^-] and thus the increased electronic conductivity, see Equation (4). Usually, titanium dioxide exhibits an n-type response to hydrogen, but some factors lead to a p-type transition, such as impurities,

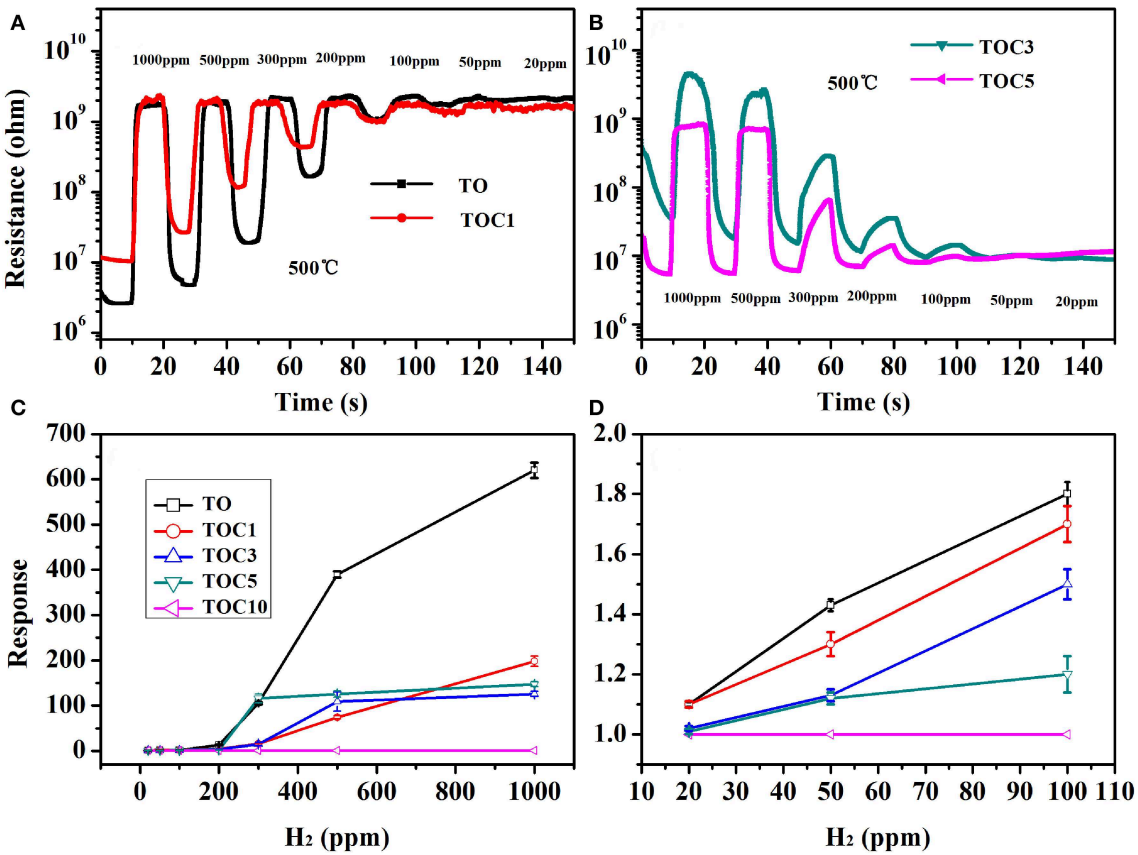

FIGURE 6 | The dynamic response curves of sensors based on TO, TOC1, TOC3, TOC5 vs. 20–1,000 ppm hydrogen at 500°C with 0.1 V applied voltage **(A,B)**. Hydrogen sensing performance (20–1,000 ppm) of TO, TOC1, TOC3, TOC5, TOC10 at 500°C with 0.1 V applied voltage **(C)**. Response values of TO, TOC1, TOC3, TOC5, TOC10 vs. 20–100 ppm hydrogen at 500°C with 0.1 V applied voltage **(D)**.

temperature, applied electric field, and gas concentration (Li et al., 2009; Haidry et al., 2018). However, contradicting with (Haidry et al., 2018), in this work the transition point and the influencing factors leading to transition were not found.

$$T<100°C: O_2\,(gas)+e^-\rightarrow O_2^-\ (ads) \quad (1)$$

$$100°C<T<300°C:\ O_2\,(gas)+2e^-\rightarrow 2O^-\,(ads) \quad (2)$$

$$T>300°C:\ \ O_2\,(gas)+4e^-\rightarrow 2O^{2-}(ads) \quad (3)$$

$$H_2+O^{2-}\rightarrow H_2O+2e^- \quad (4)$$

According to the author's best knowledge, in the temperature range of 300–500°C, pure n-type semiconductors might also show p-type response, which is resulted due to the formation of inversion layer on the surface (Li et al., 2009; Haidry et al., 2018). In detail, at the aforementioned operating temperature, strong oxygen adsorption on TiO_2 surface increases band bending greatly, also raising intergranular surface barrier. Thus, it is hard for electrons to transfer between TiO_2 grains leading to the formation of an inversion layer and holes become the majority surface charge carriers that yield a p-type sensor response. When hydrogen is supplied to the sensor surface, while the concentration of holes decreases since hydrogen reacts with adsorbed oxygen, inversion layer becomes thinner and conductivity decreases causing a p-type response. To date, the phenomenon related to the inversion layer formation and its thickness decrease is still debatable, which requires further in-deeper research.

In terms of Kroger-Vink notation, chromium may incorporate into TiO_2 lattice with 2, 3, and 6 oxide states, following Equations (5–7). Some researchers (Nowotny et al., 2016) attributed the change of the oxidation state of chromium to the increase in oxygen activity.

$$CrO\leftrightarrow Cr_{Ti}^{''}+V_{\ddot{O}}+O_O^x \quad (5)$$

$$Cr_2O_3\leftrightarrow 2Cr_{Ti}^{'}+3O_O^x+V_{\ddot{O}} \quad (6)$$

$$2CrO_3\leftrightarrow 2Cr_{\ddot{T}i}+6O_O^x+V_{Ti}^{''''} \quad (7)$$

TABLE 1 | Response and recovery time TO, TOC1, TOC3, TOC5 at 500°C (1,000 ppm).

Sample	Response time (s)	Recovery time (s)
TO	114	112
TOC1	224	130
TOC3	223	332
TOC5	142	123

With the addition of chromium dopant, the interpretation of p-type behavior is usually associated with the presence of acceptor states. Generally, chromium dopant has an effect on the electronic structure of TiO_2 and forms localized acceptor levels in the forbidden band gap. The Cr dopant in TiO_2 crystals can exist in three possible modes, isolated substitutional doping (Cr at Ti sites), substitutional doping with oxygen vacancy compensation and interstitial doping (Yang et al., 2009). On the basis of the XRD and XPS analysis, we knew that Cr can be incorporated into the lattice, as shown in reaction (8):

$$Cr_2O_3+\frac{1}{2}O_2\rightarrow 2Cr'_{Ti}+4O_O+2h* \quad (8)$$

Thus, electron holes become the dominant charge carriers. When exposed to hydrogen, the reaction between hydrogen molecular and adsorbed oxygen releases electrons making resistance increase.

CONCLUSION

In conclusion, Cr doped TiO_2 nanoparticles were successfully synthesized by sol-gel method and the hydrogen gas sensor based on TiO_2 is investigated at high temperature. Five at.% Cr doped TiO_2 gas sensor showed best gas sensing performance at 500°C. The response value is 152.65 and the response/recovery time is fast (142/123s) when it is exposed to 1,000 ppm hydrogen and it is of good selectivity to hydrogen. The results indicate that Cr doped TiO_2 synthesized by sol-gel method is promising materials for application as hydrogen gas sensor at high temperature. Cr dopant was proved to improve stability of TiO_2 gas sensor at high temperature in this work.

DATA AVAILABILITY

All datasets generated for this study are included in the manuscript and/or the supplementary files.

AUTHOR CONTRIBUTIONS

LX prepared the nanopowders and wrote this article. LS, QF, and ZW analyzed the gas sensing performance. ZL and BD carried out the characterization of the samples. AH and ZY revised, read, and approved the submitted version.

FUNDING

This research was financially supported by the Funding of Natural Science Foundation of Jiangsu Province (BK20170795) and National Natural Science Foundation of China (51850410506). This work was also supported by Opening Project from key Laboratory of Materials Preparation and Protection for Harsh Environment (56XCA17006-3) and Postgraduate Research and Practice Innovation Program of Jiangsu Province (KYCX18_0281).

REFERENCES

Alvarez, S. Y. M., Mar, J. L. G., Palomino, G. T., Alejandro, F. M., Quintero, A. C., Ramirez, A. H., et al. (2019). Synthesis of Cr^{3+}-doped TiO_2 nanoparticles: characterization and evaluation of their visible photocatalytic performance and stability. *Environ. Technol.* 40, 144–153. doi: 10.1080/09593330.2017.1380715

Asemil, M., Malekil, S., and Ghanaatshoar, M. (2017). Cr-doped TiO_2-based dye-sensitized solar cells with Cr-dopedTiO_2 blocking layer. *J. Sol-Gel Sci. Technol.* 81, 645–651. doi: 10.1007/s10971-016-4257-z

Bai, J., and Zhou, B. X. (2014). Titanium dioxide nanomaterials for sensor applications. *Chem. Rev.* 114, 10131–10176. doi: 10.1021/cr400625j

Comini, E., Ferroni, M., Guidi, V., Vomiero, A., Merli, P. G., and Morandi, V. (2005). Effects of Ta/Nb-doping on titania-based thin films for gas-sensing. *Sens. Actuators B.* 108, 18–21. doi: 10.1016/j.snb.2004.10.041

Diao, K., Huang, Y., Zhou, M., Zhang, J., Tang, Y., Wang, S., et al. (2016). Selectively enhanced sensing performance for oxidizing gases based on ZnO nanoparticle-loaded electrospun SnO_2 nano-tube heterostructures. *RSC Adv.* 6, 28419–28427. doi: 10.1039/C6RA03061K

Gonullu, Y., Haidry, A. A., and Saruhan, B. (2015). Nanotubular Cr-doped TiO_2 for use as high-temperature NO_2 gas sensor. *Sen. Actuators B.* 217, 78–87. doi: 10.1016/j.snb.2014.11.065

Haidry, A. A., Cetin, C., Kelm, K., and Saruhan, B. (2016). Sensing mechanism of low temperature NO_2 sensing with top-bottom electrode (TBE) geometry. *Sens. Actuators B.* 236, 874–884. doi: 10.1016/j.snb.2016.03.016

Haidry, A. A., Puskelova, J., Plecenik, T., Durina, P., Gregus, J., Truchly, M., et al. (2012). Characterization and hydrogen gas sensing properties of TiO_2 thin films prepared by sol-gel method. *Appl. Surf. Sci.* 259, 270–275. doi: 10.1016/j.apsusc.2012.07.030

Haidry, A. A., Sun, L. C., Saruhan, B., Plecenik, A., Plecenik, T., Shen, H. L., et al. (2018). Cost-effective fabrication of polycrystalline TiO_2 with tunable n/p response for selective hydrogen monitoring. *Sens. Actuators B.* 274, 10–21. doi: 10.1016/j.snb.2018.07.082

Hermawan, A., Asakura, Y., Kobayashi, M., Kakihana, M., and Yin, S. (2018). High temperature hydrogen gas sensing property of GaN prepared from α-GaOOH. *Sens. Actuators B.* 276, 388–396.doi: 10.1016/j.snb.2018.08.021

Jing, Z. H., Ling, B. P., Yu, Y., Qi, W., and Zhang, S. F. (2015). Preparation and gas sensing activity of La and Y co-doped titania nanoparticles. *J. Sol-Gel Sci. Techn.* 73, 112–117. doi: 10.1007/s10971-014-3501-7

Lacz, A., Lancucki, L., Lach, R., Kamecki, B., and Drozdz, E. (2018). Structural and electrical properties of Cr-doped $SrTiO_3$ porous materials. *Int. J. Hydrogen Energy.* 43, 8999–9005. doi: 10.1016/j.ijhydene.2018.03.180

Li, X. G., Ramasamy, R., and Dutta, P. K. (2009). Study of the resistance behavior of anatase and rutile thick films towards carbon monoxide and oxygen at high temperatures and possibilities for sensing applications. *Sens. Actuators B* 1, 308–315. doi: 10.1016/j.snb.2009.09.021

Li, Z., Haidry, A. A., Wang, T., and Yao, Z. J. (2017). Low-cost fabrication of highly sensitive room temperature hydrogen sensor based on ordered mesoporous Co-doped TiO_2 structure. *Appl. Phys. Lett.* 111:032104. doi: 10.1063/1.4994155

Li, Z., Yao, Z. J., Haidry, A. A., Plecenik, T., Xie, L. J., Sun, L. C., et al. (2018). Resistive-type hydrogen gas sensor based on TiO_2: a review. *Int. J. Hydrogen Energy*. 43, 21114–21132. doi: 10.1016/j.ijhydene.2018.09.051

Liu, Y. X., Parisi, J., Sun, X. C., and Lei, Y. (2014). Solid-state gas sensors for high temperature applications–a review. *J. Mater. Chem. A*. 2, 9919–9943. doi: 10.1039/C3TA15008A

Low, I. M., Albetran, H., Prida, V. M., Vega, V., Manurung, P., and Ionescu, M. (2013). A comparative study on crystallization behavior, phase stability, and binding energy in pure and Cr-doped TiO_2 nanotubes. *J Mater. Res*. 28, 304–312. doi: 10.1557/jmr.2012.275

Luo, Y. F., Zhang, C., Zheng, B. B., Geng, X., and Debliquy, M. (2017). Hydrogen sensors based on noble metal doped metal-oxide semiconductor: a review. *Int. J. Hydrogen Energy* 42, 20386–20397. doi: 10.1016/j.ijhydene.2017.06.066

Lyson-Sypien, B., Czapla, A., Lubecka, M., Gwizdz, P., Schneider, K., Zakrzewska, K., et al. (2012). Nanopowders of chromium doped TiO_2 for gas sensors. *Sens. Actuators B*. 175, 163–172. doi: 10.1016/j.snb.2012.02.051

Monamary, A., Vijayalakshmi, K., DavidJereil, S. (2019). Hybrid Cr/TiO_2/ITO nanoporous film prepared by novel two step deposition for room temperature hydrogen sensing. *Physica B*. 553, 182–189. doi: 10.1016/j.physb.2018.10.049

Nowotny, J., Macyk, W., Wachsman, E., and Rahman,. K. (2016). Effect of oxygen activity on the n-p transition for pure and Cr doped TiO_2. *J. Phys. Chem. C*. 120, 3221–3228. doi: 10.1021/acs.jpcc.5b12101

Pan, F. J., Lin, H., Zhai, H. Z., Miao, Z., Zhang, Y., Xu, K. L., et al. (2018). Pd-doped TiO_2 film sensors prepared by premixed stagnation flames for CO and NH_3 gas sensing. *Sens. Actuators B*. 261, 451–459. doi: 10.1016/j.snb.2018.01.173

Peng, Y. H., Huang, G. F., and Huang, W. Q. (2012). Visible-light absorption and photocatalytic activity of Cr-doped TiO_2 nanocrystal films. *Adv. Powder Technol*. 3, 8–12. doi: 10.1016/j.apt.2010.11.006

Sennik, E., Alev, O., and Ozturk, Z. Z. (2016). The effect of Pd on the H_2 and VOC sensing properties of TiO_2 nanorods. *Sens. Actuators B*. 229, 692–700. doi: 10.1016/j.snb.2016.01.089

Sun, L. C., Yao, Z. J., Haidry, A. A., Li, Z., Fatima, Q., and Xie, L. J. (2018). Facile one-step synthesis of TiO_2 microrods surface modified with Cr_2O_3 nanoparticles for acetone sensor applications. *J. Mater. Sci*. 29, 14546–14556. doi: 10.1007/s10854-018-9589-8

Yamazoe, N., and Shimanoe, K. (2008). Theory of power laws for semiconductor gas sensors. *Sens. Actuators B*. 128, 566–573. doi: 10.1016/j.snb.2007.07.036

Yang, K., Dai, Y., and Huang, B. B. (2009). Density functional characterization of the electronic structure and visible-light absorption of Cr-doped anatase TiO_2. *Chem. Phys. Chem*. 10, 2327–2333. doi: 10.1002/cphc.200900188

Conflict of Interest Statement: The authors declare that the research was conducted in the absence of any commercial or financial relationships that could be construed as a potential conflict of interest.